Appendix E
FCT Document Cover Sheet

Name/Title of Deliverable/Milestone: PNNL REPOSITORY SCIENCE/ WASTE FORM DEGRADATION: PROGRESS REPORT

Work Package Title and Number: UFD Repository Sciences Waste Form Degradation and Radionuclide Release – FTPN11UF0336-PNNL

Work Package WBS Number: 1.02.08.03 Milestone Number: M31UF033601

Responsible Work Package Manager: Edgar Buck (Name/Signature) 7/15/2011 (Date Submitted)

Quality Rigor Level for Deliverable/Milestone	☒ QRL-3	☐ QRL-2	☐ QRL-1 ☐ Nuclear Data	☐ N/A*

This deliverable was prepared in accordance with Pacific Northwest National Laboratory
(Participant/National Laboratory Name)

QA program which meets the requirements of
☒ DOE Order 414.1 ☐ NQA-1-2000 ☐ Other:

This Deliverable was subjected to:
☒ Technical Review ☐ Peer Review

Technical Review (TR)
Review Documentation Provided
☐ Signed TR Report, or
TR Report No.:
☐ Signed TR Concurrence Sheet (attached), or
☒ Signature of TR Reviewer(s) below

Peer Review (PR)
Review Documentation Provided
☐ Signed PR Report, or
PR Report No.:
☐ Signed PR Concurrence Sheet (attached), or
☐ Signature of PR Reviewers below

Name and Signature of Reviewers

(Name/Signature)	(Date)
Charles Soderquist	7/15/2011

*Note: In some cases there may be a milestone where an item is being fabricated, maintenance is being performed on a facility, or a document is being issued through a formal document control process where it specifically calls out a formal review of the document. In these cases, documentation (e.g., inspection report, maintenance request, work planning package documentation, or the documented review of the issued document through the document control process) of the completion of the activity along with the Document Cover Sheet is sufficient to demonstrate achieving the milestone. QRL for such milestones may also be marked N/A in the work package provided the work package clearly specifies the requirement to use the Document Cover Sheet and provide supporting documentation.

REPOSITORY SCIENCE/ WASTE FORM DEGRADATION: PROGRESS REPORT

Fuel Cycle Research & Development
Used Fuel Disposition

Prepared for
U.S. Department of Energy
Used Fuel Disposition Campaign
E. C. Buck, R.S. Wittman, J. W. Hayes, S. M. Kiser
Pacific Northwest National Laboratory

July, 2011
FCRD-USED-2011-000213

SUMMARY

The purpose of the proposed Used Fuel Disposition (UFD) testing program at Pacific Northwest National Laboratory (PNNL) is to improve understanding of the corrosion of spent nuclear fuel (or Used Fuel) and the potential for radionuclide (RN) release within reducing and anoxic environments. The role of reducing fronts, corrosion of potential waste package materials, the role of radiolysis, secondary phases and radionuclide migration either as solutes or colloids will be important for developing defensible models for generic geologic disposal environments.

It is well understood that uraninite (UO_2) is stable under reducing conditions; however, even natural uraninite deposits in reducing environments have experienced some alteration. In the case of Used Fuel, the main driver for the alteration at the fuel surface will be radiolysis of any contacting water or water vapor. Once solubilized, uranium may precipitate at the reducing front; however, radionuclides may or may not be sequestered at the reducing front. New insights into the behavior of I, Se, Np, and Tc at the reducing front may have high impact on dose driven performance assessment models. Indeed, the behavior of this system may also be inherently more complex than that of an oxidizing environment as localized oxidizing fields may have an impact on RN solubility. Initially, the local β,γ-radiolytic field will dominate the repository (depending on the timing of emplacement) but later α-radiolysis will control the radiolytic field. The strength of this field will depend on burn-up, presence of other materials, and the exposed surface area. Radiolysis should be greater for high burn-up and/or mixed oxide (MOX) fuels.

Radiolysis results in the build-up of H_2O_2 at the fuel surface as well as the formation of H_2 and O_2. The role of other materials in the repository, such as Zircaloy and iron-based waste packages, will be extremely important as these metals may oxidize and release further H_2 or form hydrides. For instance, Spent Fuel corrosion rates are known to decrease with H_2 over-pressure (Carbol et al. 2009); however, if H_2 is removed from the Engineered Barrier System (EBS) or if zirconium acts as a sink for hydrogen, this effect could decrease. To address these issues, radiolysis simulations have been developed to model the possible processes that may occur in a generic EBS with Used Fuel. The model developed has been validated by comparison with the literature; however, experiments will be required to validate the more complex systems. The overall objective will be to provide a more complete picture of fuel degradation in a reducing geologic disposal environment.

Predicted dissolved uranium concentration taken from the Christensen and Shoesmith (1994) kinetics data sets were adapted to the experimental conditions of the Single Pass Flow-Through (SPFT) test columns as presented by Gray et al. (1992). These SNF tests used the Approved Testing Material (ATM)-103 Spent Nuclear Fuel. The idealized model predictions showed a steady state concentration of radiolytic products

(e.g. H_2O_2) and dissolved uranium within several hours. We found that the measured dissolution rates of approximately 6 mg/d•m^2 of Gray et al. (1992) required a localized dose rate of about 50 Gy/hr which was consistent with the ^{137}Cs gamma dose expected from the 33 MWd/kgU Spent Fuel with a 10 yr decay time. Dose dependent modeling results were compared to the dissolution rates reported by Gray et al. (1992). We find good evidence that previously reported dissolution rates for SNF were mainly due to β,γ-radiolysis and, hence, were artifacts of the relatively young age of the tested material. It is not possible to avoid these effects with laboratory tests with SNF.

Understanding and modeling these processes will lead to a scientific basis for reductions in predicted degradation rates and radionuclide immobilization. This could provide a significant benefit to the disposal program in terms of estimated dose reduction.

CONTENTS

FIGURES

ACRONYMS AND ABBREVIATIONS

ANL	Argonne National Laboratory
ATM	Approved Testing Material
DR	Dissolution rate
EBS	Engineered Barrier System
$e_{(aq)}$	Aqueous Electron
FACSIMILE	A computer program for modeling the kinetics of chemical systems
FCRD	Fuel Cycle Research and Development
FeO_x	Iron oxide hydroxide corrosion products
LET	linear energy transfer
LLNL	Lawrence Livermore National Laboratory
MOX	Mixed oxide fuel
ODEPACK	Computer codes for ordinary differential equations
PNNL	Pacific Northwest National Laboratory
RN	Radionuclide
S_A	surface area (m^2)
SEM	Scanning Electron Microscopy
SNF	Spent Nuclear Fuel
SPFT	Single pass flow-through test
UFD	Used Fuel Disposition

MINERAL NAMES AND FORMULAE

Coffinite	$USiO_4$
Ferrihydrite	$Fe_5O_3(OH)_9$ (more commonly written as FeOOH)
Goethite	α-FeOOH
Hematite	Fe_2O_3
Meta-schoepite	$[(UO_2)_4O(OH)_6](H_2O)_5$
Meta-studtite	$UO_4 \cdot 2H_2O$
Schoepite	$[(UO_2)_8O_2(OH)_{12}](H_2O)_{12}$
Studtite	$[(UO_2)\ O_2(H_2O)_2](H_2O)_2$
Uraninite	UO_2

UNITS

μm	micrometer
Gy	Grays (100 Rads)

M	molarity, mole/liter
mg	milligram

Repository Science/waste form degradation: Progress Report

1. Introduction

The purposes of the waste form testing and radiolysis modeling program at Pacific Northwest National Laboratory (PNNL) is to improve understanding of corrosion mechanisms and the fate of radionuclides. The Light Water Reactor Spent (Used) UO_2 Fuel matrix is the first barrier within any proposed geologic repository design. This material is known to possess high stability in an anoxic environment. Hence, the essential parameter to describe the long-term stability of Spent (Used) Fuel in the Engineered Barrier System (EBS) of a generic repository is the local oxidizing potential (Eh) and the ability for oxidants to oxidize UO_2. Because of the internal radioactivity of the Used Fuel and the anoxic or reducing EBS, a dynamic redox system will be generated at the fuel/water/air interface from water radiolysis. A schematic of these processes is shown in Figure 1.1. This project aims to model the formation of oxidants and reductants at the fuel surface in a complex and changing environment, to make predictions about this environment, and to provide fundamental experimental data to support long-term scientifically defensible models.

1.1 Work Activities at PNNL

- PNNL Task 1 (FTPN11UF0336) – Evaluation of Radiolysis Models to Used Fuel Degradation and Radionuclide Migration in a Degraded EBS Environment.
- PNNL Task 2 (FTAN11UF0336) – Development of Simulant Fuels for Experimental Investigation of Used Fuel Degradation at Future Conditions.

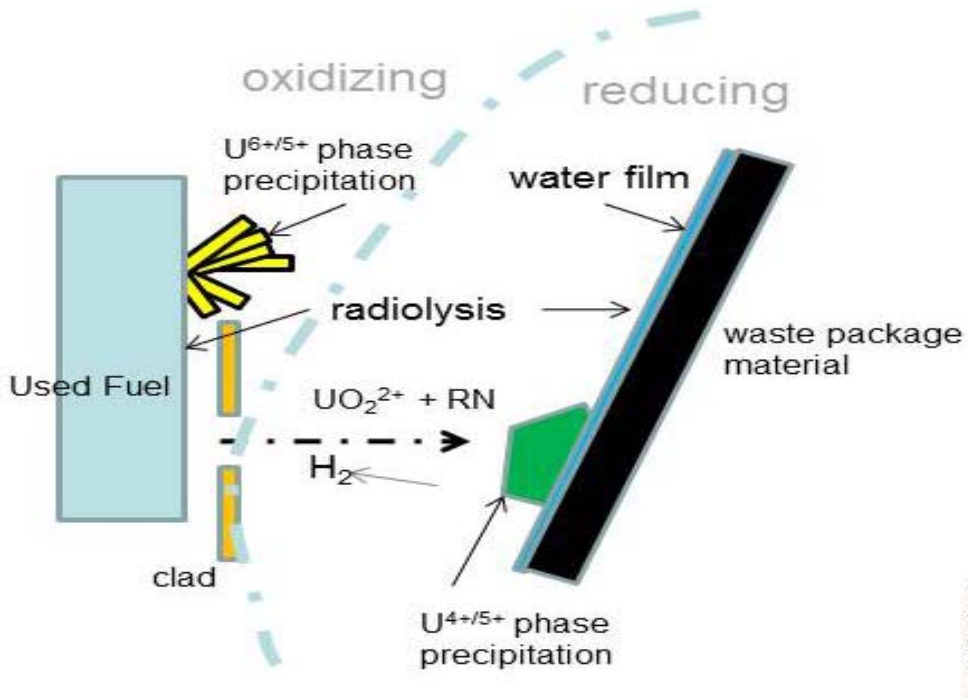

Figure 1.1 Schematic diagram showing processes concerned with the corrosion of Used Fuel in a reducing environment

A high-level waste repository environment will be a dynamic redox system because of the time-dependent generation of radiolytic oxidants and reductants and the corrosion of Zr- and Fe-bearing canister materials (Spahiu et al. 2002; Pérez del Villar et al. 2002; Carbol et al. 2009). A major difference between Spent (Used) Fuel and natural analogues, including unirradiated UO_2, is the intense radiolytic field. The radiation emitted by SNF can produce radiolysis products (including OH• and H• radicals, O_2^-, $e^-_{(aq)}$, H_2O_2, H_2, and O_2) that will increase the waste form degradation rate and change radionuclide behavior. As H_2 escapes from the water layer surface, the local conditions at the fuel/water interface should always be oxidizing in the α-radiolytic field even in reducing environments (see Table 1.1). Experiments with fresh UO_2 based fuel are significantly influenced by their high β,γ-radiation field that results in generation of powerful radiolytic species (e.g., OH• and H_2O_2) at the fuel/water interface. It is probably highly conservative to use rates of reaction from fresh (or even 30 yr old) Spent (Used) Fuel for performance assessment calculations. After 300 to1000 years, the β/γ-radiolytic field will be reduced by three orders of magnitude, and the rate of dissolution will decrease significantly. Data are needed to establish the magnitude of this effect; however, it is important to run such tests with materials that are truly comparable. This requires the use of well-characterized solids where the chemistry, morphology, and grain size are kept constant, as are the testing conditions, and where the only variable is the radiation field.

Table 1.1 Comparison of G-values for gamma and alpha radiolysis

Species	G-value	
	Gamma	Alpha
OH	2.67	0.24
e_{aq}	2.66	0.06
H^+	2.76	0.30
H	0.55	0.21
H_2	0.45	1.3
H_2O_2	0.72	0.985
OH^-	0.1	0.02
H_2O	-6.87	-2.71

Controlled experiments by Bruno et al. (2002) lead to the establishment of effective G-values for H_2O_2 generation that consider the effect of iron and UO_2 surfaces. These approaches will lead to less conservative predictions for spent fuel dissolution, but these models and experiments are not always relevant to all possible repository environments. By measuring radiolytic generation rates with α-doped UO_2 under various conditions, critical radiolysis data can be obtained that will improve models. Hughes-Kubatko et al. (2003) estimated generation rates for H_2O_2 on the surface of natural uraninite covered with

a thin film of water. New mixed potential models are now looking at α-emitters concentrated at the fuel surface. Under stagnant water conditions or thin water films, α-radiolysis may have a significant impact on the local oxidation potential.

King et al. (1999) have developed an electrochemical model for predicting the effects of α-radiolysis, the precipitation of uranyl secondary minerals, and redox processes with Fe(0) and Fe(II) on the dissolution of UO_2. Radical reactions were not considered in the model in the 1999 version of the mixed potential model. The total amount of radiolytic products decreases with linear energy transfer (LET) due to back reactions. Radiolytic products are generated in spurs. At high LET (i.e. α-radiolysis), the spurs are densely packed, and very fast secondary reactions occur resulting in a loss of radicals and an increase in molecular products. However, in more complex media, many other reactions can occur that will significantly impact radiolytic species. Every reaction of $e^-_{(aq)}$, H•, and OH• produces secondary radical products. These radicals can react with other species in the fuel cell environment to produce other reactive species such as CO_3^-, CO_2^-, Cl_2^-, I_2^-, if C, Cl, or I are present. Christensen and Sunder (2000) have determined that the diffusion length for radicals depends weakly on inverse dose. For instance, at a dose of 280 Gy•hr^{-1} the OH• range is 16 μm, and at 5 Gy•hr^{-1} the range is 44 μm.

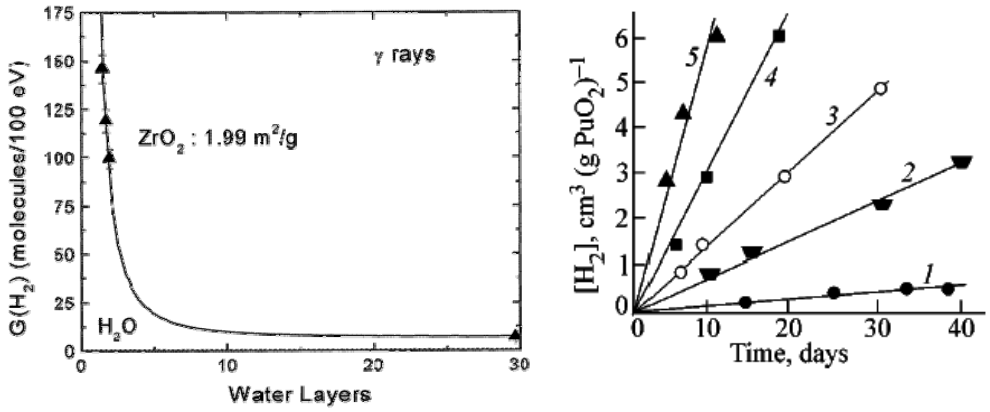

Figure 1.2 Effect of Water Content on G(H_2). Data taken from (a) LaVerne and Tandon (2002) and (b) Vladimirova and Kulikov (2002). The number of water layers in (a) was calculated based on water content in the test. Water content in (b) decreases from 3%(marked as 5 on the figure) to 0.3% (marked as 1 on the figure).

The production rates of H_2 and other radiolytic products may be enhanced by the various oxide surfaces in the waste package or EBS. It is thought that the surface radiolytic enhancement process must depend on the oxide electronic structure and on the energetics and geometric structures of the adsorbed species. The effect of oxide surfaces have been demonstrated through increasing H_2 generation with increasing surface area of a non-radioactive component by LaVerne and co-workers at Notre Dame University (see Pastina and LaVerne (2001) and LaVerne and Tandon (2002)).

LaVerne and Tandon (2002) have demonstrated that H_2 generation is increased significantly in a vapor environment (See Figure 1.2a); although Vladimirova and Kulikov (2002) apparently show an opposite effect (See Figure 1.2b), where increasing amounts of water resulted in greater H_2 production. However, the total amount of water in the system was still low and the lower water content tests by Vladimirova and Kulikov (2002) may have been limited water removal from the actinide surface. Band gap energy is a fundamental parameter that affects various radiation-induced processes on the surfaces of insulators and semi-conductors (Petrik et al. 2001) (see Figure 1.3).

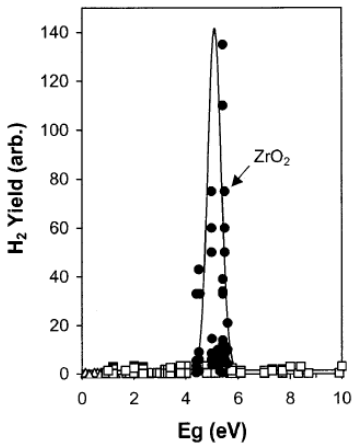

Figure 1.3 Hydrogen yield versus oxide band gap for the radiolysis of water. [Data taken from Petrik, N. G. et al. (2001)]

The energy of the H-OH bond in the water molecule is 5.1 eV. However, the dissociative excitation thresholds in vapor and physic-sorbed water are higher, near to 7.45eV (Petrik et al. 2001).

2. Radiolysis Modeling

Radiolysis studies have shown that the combination of β and γ radiolysis is particularly aggressive, accounting for very high corrosion potentials, and may lead to exaggerated release of Tc and actinides (Sunder et al. 1997; Shoesmith 2000). Radiolysis effects from fresh fuel will modify the local redox conditions and therefore the speciation and the solubility of fuel. The high β,γ dose rates from fresh fuel (i.e. 10-20 year old fuel) will generate local acidity (from nitric acid formation in air (Gray and McVay, 1985)) as well as high oxidation (Eh) potentials. Acidity may also lead to grain boundary attack leading to preferential release of radionuclides in these regions. These effects have been observed in corrosion tests on the unsaturated drip tests on spent fuel, including release of Tc (Finn et al. 1998), corrosion of grain boundaries (Finch et al. 1999), and unusual behavior in the actinides (Buck et al. 2004). Shoesmith (2000) has suggested that grain boundary disintegration and Tc release observed in the SNF drip tests is entirely due to the intense β,γ-field. Experimentally, it is difficult to separate the spurious β,γ-field from the long-lived α-field; hence, computational modeling of these processes may be extremely important for understanding long term behavior in a generic repository.

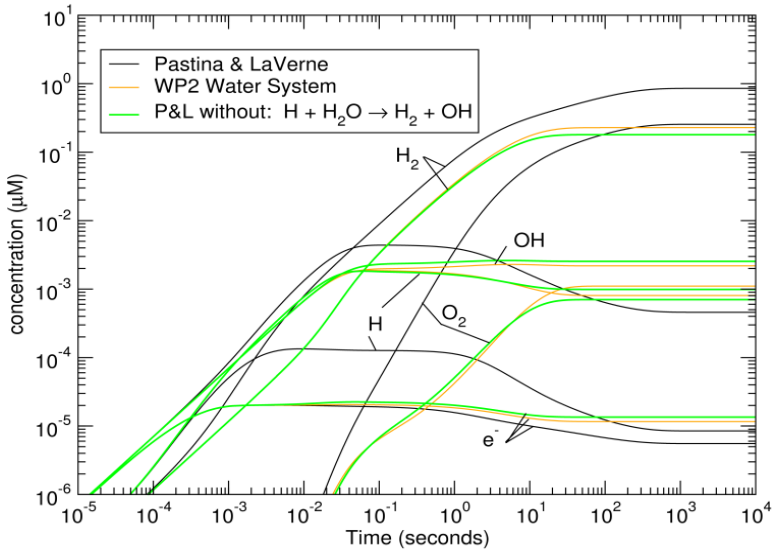

Figure 2.1 Predicted Hydrogen and Oxygen Production Rates in a Static Configuration.

Several research groups have modeled water radiolysis, including Li and Olander (1999) and Pastina and LaVerne (2001). Pastina and LaVerne (2001) have published predictive models for water radiolysis that are illustrated in Figure 2.1. In this figure, computational simulations from Pastina and LaVerne (2001) have been compared against the models developed in this study with good results. The Pastina and LaVerne (2001) modeled 79 equations using the commercially available FACSIMILE code. It is

debateable whether all reactions are equally important and, indeed, Li and Olander (1999) developed a similar predictive model but limited the series of elementary reactions to examine the production rates of H_2, O_2, and H_2O_2 in water exposed to an alpha source. The total number of reactions used in the Li and Olander (1999) model was reduced from the 79 elementary reactions described by Pastina and LaVerne (2001) to eleven reactions. The G-values for H•, OH•, and H_2 for initial conditions were 7.4, 6.2, and 0.5, respectively and included a rate, k_d, term for the decomposition of H_2O_2. The rate for k_d is temperature dependent. The removal of other possible reactions may lead to errors in using this reaction scheme for the fuel cell configurations. For example, in Figure 2.1, when the $\bullet H + H_2O \rightarrow H_2 + \bullet OH$ reaction was excluded, the PNNL developed model matched the Pastina and LaVerne (2001) results.

Table 2.1 List of Equations used in the Water Radiolysis System (taken from Poinssot et al. (2005); Christensen and Sunder, 2000)

Water System Reactions	Rate Constants (M-s)$^{-1}$
H+ + OH- = H2O	1.43E11
H2O = H+ + OH-	2.574E-5
H2O2 = H+ + HO2-	3.56E-2
H+ + HO2- = H2O2	2.0E10
E- + H2O = H + OH-	2.E1
H + OH- = E- + H2O	1.5E7
E- + H+ = H	2.2E10
OH + OH- = O- + H2O	1.2E10
O- + H2O = OH + OH-	9.3E7
HO2 = O2- + H+	8.0E5
O2- + H+ = HO2	4.5E10
E- + OH = OH-	3.0E10
E- + H2O2 = OH + OH-	1.2E10
E- + O2- + H2O = HO2- + OH-	1.3E10
E- + O2 = O2-	1.9E10
E- + H + H2O = H2 + OH-	2.5E10
E- + HO2- = O- + OH-	3.5E9
H + H = H2	1.E10
H + OH = H2O	2.0E10
H + H2O2 = OH + H2O	6.0E7
H + O2 = HO2	1.8E10
H + HO2 = H2O2	2.0E10
H + O2- = HO2-	2.0E10
OH + OH = H2O2	5.5E9
OH + HO2 = H2O + O2	7.9E9
OH + O2- = OH- + O2	9.0E9
OH + H2 = H + H2O	3.4E7
OH + H2O2 = HO2 + H2O	2.7E7
OH + HO2- = HO2 + OH-	5.0E9
HO2 + O2- = HO2- + O2	9.6E7
HO2 + HO2 = H2O2 + O2	8.4E5
H2O2 = H2O + O	1.0E-3

O + O = O2	1.0E9
Carbonate System Reactions	**Rate Constants (M-s)$^{-1}$**
H+ + CO3-2 = HCO3-	5.0E10
CO2 + H2O = H+ + HCO3-	7.0E1
H+ + HCO3- = CO2 + H2O	1.0E10
HCO3- = CO3-2 + H+	2.0E00
CO2 + E- = CO2-	7.7E09
HCO3- + OH = CO3- + H2O	8.5E06
CO3-2 + OH = CO3- + OH-	3.9E08
HCO3- + H = H2 + CO3-	4.4E04
CO3-2 + E- = CO2- + OH- + OH- - H2O	3.9E05
CO3- + CO3- = C2O6-2	1.4E07
CO3- + H2O2 = CO3-2 + O2- + H+ + H+	9.8E05
CO3- + HO2- = CO3-2 + O2- + H+	1.0E07
CO3- + O2- = CO3-2 + O2	4.0E08
CO3- + CO2- = CO3-2 + CO2	3.0E08
CO2- + E- = HCOO- + OH- - H2O	1.0E09
CO2- + CO2- = C2O4-2	6.5E08
CO2- + O2 = CO2 + O2-	2.0E09
CO2- + H2O2 = CO2 + OH- + OH	7.3E05
CO2- + HCO3- = HCOO- + CO3-	1.0E03
C2O6-2 = C2O4-2 + O2	1.0E00
C2O6-2 = HO2- + OH- + CO2 + CO2 - H2O	2.0E02
CO3- + C2O4-2 = C2O4- + CO3-2	3.0E03
C2O4-2 + E- = C2O4-3	3.1E07
C2O4-2 + OH = C2O4- + OH-	7.7E06
CO3- + HCOO- = HCO3- + CO2-	1.5E05
HCOO- + OH = H2O + CO2-	3.2E09
HCOO- + H = H2 + CO2-	2.1E08
HCOO- + E- = H2 + CO2- - H+	8.0E08
OH- + HCO3- = CO3-2 + H2O	1.0E09
CO3-2 + H2O = OH- + HCO3-	3.6E03
CO3- + CO3- = CO4-2 + CO2	7.0E06
H2O + CO4-2 = HO2- + CO2 + OH-	2.0E-1
Chloride System Reactions	**Rate Constants**
OH + Cl- = ClOH-	4.300E+09
OH + HClO = ClO + H2O	9.000E+09
OH + ClO2- = ClO2 + H2O - H+	6.300E+09
E- + Cl = Cl- + H2O	1.000E+10
E- + Cl2- = Cl- + Cl- + H2O	1.000E+10
E- + ClOH- = Cl- + OH- + H2O	1.000E+10
E- + HClO = ClOH-	5.300E+10
E- + Cl2 = Cl2-	1.000E+10
E- + Cl3- = Cl2- + Cl-	1.000E+10
E- + ClO2- = ClO + OH- - H+	4.500E+10
E- + ClO3- = ClO2 + OH- - H+	0.000E+00
H + Cl = Cl- + H+	1.000E+10
H + Cl2- = Cl- + Cl- + H+	8.000E+09
H + ClOH- = Cl- + H2O	1.000E+10
H + Cl2 = Cl2- + H+	7.000E+09
H + HClO = ClOH- + H+	1.000E+10
H + Cl3- = Cl2- + Cl- + H+	1.000E+10

HO2 + Cl2- = Cl- + HCl + O2	4.000E+09
HCl = Cl- + H+	5.000E+05
HO2 + Cl2 = Cl2- + H+ + O2	1.000E+09
HO2 + Cl3- = Cl2- + HCl + O2	1.000E+09
O2- + Cl2- = Cl- + Cl- + O2	1.200E+10
O2- + HClO = ClOH- + O2	7.500E+06
H2O2 + Cl2- = HCl + HCl + O2-	1.400E+05
H2O2 + Cl2 = HO2 + Cl2- + H+	1.900E+02
H2O2 + HClO = HCl + H2O + O2	1.700E+05
OH- + Cl2- = ClOH- + Cl-	7.300E+06
OH- + Cl2 = HClO + Cl-	1.000E+10
H+ + ClOH- = Cl + H2O	2.100E+10
H2O + Cl2O2 = HClO + ClO2- + H+	2.000E+02
H2O + Cl2O2 = O2 + HClO + HCl	0.000E+00
H2O + Cl2O = HClO + HClO	1.000E+02
H2O + Cl2O4 = ClO2- + ClO3- + H+ + H+	1.000E+02
H2O + Cl2O4 = HClO + HCl + O4	1.000E+02
O4 = O2 + O2	1.000E+05
Cl- + Cl = Cl2-	2.100E+10
Cl- + ClOH- = Cl2- + OH-	9.000E+04
Cl- + HClO = Cl2 + OH-	6.000E-02
Cl- + Cl2 = Cl3-	1.000E+04
Cl- + H+ = HCl (assuming pKa = -3.9)	6.295E+01
ClOH- = OH + Cl-	6.100E+09
Cl2- = Cl + Cl-	1.100E+05
Cl2- + Cl2- = Cl3- + Cl-	7.000E+09
Cl3- = Cl2 + Cl-	5.000E+04
ClO + ClO = Cl2O2	1.500E+10
ClO2 + ClO2 = Cl2O4	1.000E+02
Cl2O2 + ClO2- = ClO3- + Cl2O	1.000E+02
E- + ClO3- = ClR--	1.600E+05
ClR-- + OH = OH- + ClO3-	1.000E+10
ClR-- + O- = OH- + ClO3- - H+	1.200E+09
HClO + HClO = Cl- + ClO2- + H+ + H+	6.000E-09
ClO2- + HClO = Cl- + ClO3- + H+	9.000E-07
HClO + HClO = O2 + HCl + HCl	3.000E-10
HClO4 = H+ + ClO4-	1.000E+10
H+ + ClO4- = HClO4	1.000E+03

Table 2.1 includes reaction rate data for salt environments. These are an important set of equations for the generic salt dome repository environment that will be investigated in the future.

2.1 Program Development

The system of ordinary differential equations (ODE) derived from the chemical reaction equations as shown in Table 2.1 can be fed into a fourth order Runge-Kutta algorithm to produce simulated concentration profiles of the radiolysis species (H_2O_2, H_2, etc.) as well as oxygen. Because of the need to model the system for long time periods (several hours); the initial small errors in the simulation may be

propagated into large errors. At PNNL, a collection of FORTRAN solvers was used in the radiolytic model, termed, ODEPACK that were designed for ODE problems (published by Lawrence Livermore National Laboratory (LLNL)). Information on these is available at http://people.sc.fsu.edu/~jburkardt/f77_src/odepack/odepack.html . The package consists of nine solvers which are suitable for both stiff and non-stiff systems. It included solvers for systems given in explicit form, $dy/dt = \mathbf{f}(t,y)$, and also solvers for systems given in linearly implicit form, $\mathbf{A}(t,y)\, dy/dt = \mathbf{g}(t,y)$. Initial attempts at this problem resulted in some instabilities which were eliminated by using the ODEPACK codes.

To make predictions on the dissolution of UO_2, the techniques of Christensen and Sunder (2000) were adopted. This required the inclusion of several additional equations, involving UO_2 and its reaction with H_2O and other species (see Table 2.2). In the Christensen and Sunder model, to predict UO_2 fuel oxidation rates due to water radiolysis, the thickness of the water layer was assumed to be equivalent to the diffusion path of the radicals formed during radiolysis. This limits the range that radicals can travel and leads to the molecular radiolytic species dominating reaction kinetics. Christensen and Sunder (2000) created two types of dummy species, the first termed UO_3D represented UO_3 (more correctly UO_2^{2+}) diffusing out of the reaction layer near the UO_2 surface. This removal may be complete dissolution or it could represent the precipitation of a secondary phase. The UO_2D species represented another imaginary species that was used to maintain the supply of UO_2 in the reaction layer.

Table 2.2 List of Equations used in the Water-UO_2 Radiolysis System

Uranium System Reactions	Rate Constants
UO2 = UO2D	7.0E-4
UO2D = UO2	3.5E-7
UO3 = UO3D	4.0E-4
UO2 + OH = UO3H	4.0E+8
UO2 + H2O2 = UO3H + OH	2.0E-1
UO2 + HO2 = UO3H + H2O2 - H2O	2.0E+8
UO2 + O2- = UO3H + HO2- - H2O	2.0E+8
UO3H + UO3H = UO3 + UO2 + H2O	1.0E-1
UO3H + OH = UO3 + H2O	8.0E+8
UO3H + E- = UO2 + OH-	5.0E+8
UO3H + H2O2 = UO3 + H2O + OH	2.0E-1
UO3H + O2- = UO3 + HO2-	4.0E+8
UO3H + HO2 = UO3 + H2O2	4.0E+8
UO3 + E- = UO3H + OH- - H2O	5.0E+8
UO3 + O2- = UO3- + O2	4.0E+7
UO3- + H2O = UO3H + OH-	1.0E+1
UO3H + H = UO2 + H2O	4.5E+6
UO3 + H = UO3H	4.5E+6
UO3 + HO2 = UO3H + O2	4.0E+7
UO2 + O2 = UO3H + HO2 - H2O	1.0E-3

UO3H + O2 = UO3 + HO2	1.0E-3
UO2 + CO3- = UO3H + HCO3- - H2O	4.00E8
UO3H + CO3- = UO3 + HCO3-	8.00E8

2.2 Peroxide Decomposition

In Figure 2.2, the results of examining H_2O_2 decomposition are illustrated. H_2O_2 is the most important radiolytic oxidant. The stability of H_2O_2 is an important criterion when considering long term alteration effects.

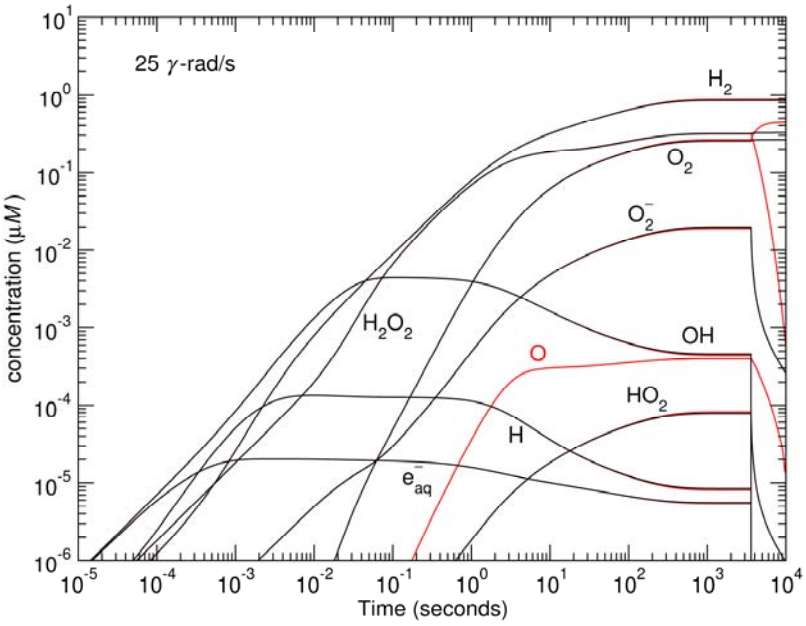

Figure 2.2 Effect of Hydrogen Peroxide Decomposition

The radiation dose from natural uraninite (UO_2) would not be considered sufficient to generate enough H_2O_2 to result in the formation of studtite ($[(UO_2)\ O_2(H_2O)_2](H_2O)_2$) and meta-studtite ($UO_4 \bullet 2H_2O$); however, examination of geologic analogs have confirmed the occurrence of these minerals at the uranium deposit at Shinkolobwe, Zaire (Finch and Ewing, 1992) and at other sites. The mineral has been found on the surface of spent fuel (Hanson et al. 2005). The presence of iron oxide corrosion products with an Engineered Barrier System (EBS), such as; ferrihydrite ($Fe_5O_3(OH)_9$), goethite (α-FeOOH), and/or hematite (Fe_2O_3), may catalyze the decomposition of H_2O_2 preventing significant build-up over time of peroxide. The decomposition conditions (red-lines) were for the $H_2O_2 \rightarrow H_2O + O$ reaction listed in Table 2.1 as 1×10^{-3}. The radiation field was 'turned-off' at 1 hr showing the stability of species in the absence of H_2O_2 decomposition. With peroxide decomposition, the concentration of O_2 increases until the

supply of H_2O_2 is exhausted. The occurrence of studtite and meta-studtite in nature is evidence of extremely stable conditions for peroxide.

2.3 Water-Carbonate Reaction

The complex behavior of carbonate in the radiolysis is shown in Figure 2.3. In this case, the 'UO_2' was placed into solution. No multiple layer systems were involved in the simulation. This simulation was run as a check on how the model responded.

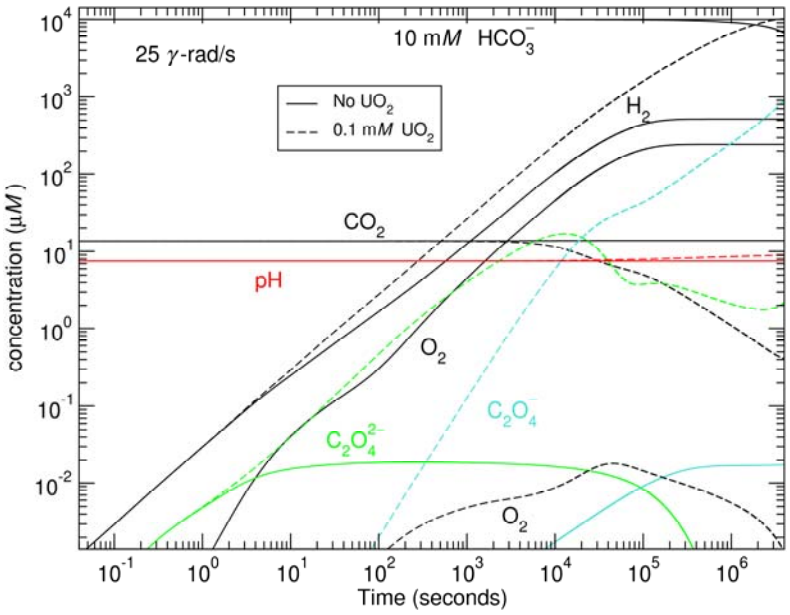

Figure 2.3 Simulation of radiolytic products in a carbonate environment in the presence and absence of UO_2

Figure 2.3 shows radiolysis induced concentrations for a 10mM HCO_3^- solution without UO_2 present (solid lines) and with UO_2 present (dashed lines) fixed at 0.1 mM. This was the UO_2 concentration assumed in the European Spent fuel program (Poinssot et al. 2005). The oxalate formation is coming mainly from the $2CO_2^- \rightarrow C_2O_4^{2-}$, where the unique species, CO_2^- is produced from the reaction of the aqueous electron ($e_{(aq)}$) and CO_2. For some reason the very small $e_{(aq)}$ concentration continues to increase with time when the UO_2 is present. The presence of UO_2 is leading to significant quantities of oxalate in the system. This has not been reported previously. As more species and reactions are added to the current radiolysis model, we are seeing many more complicated effects that will require experimental validation. The occurrence of oxalate is interesting as this is a species that can be measured in solution with infrared or Raman methods and does not have the leaking problems associated with accurately measuring H_2, for instance. In Figure 2.4, the formation of various oxalate species in the presence of

irradiated carbonate-bicarbonate solutions is shown. The radiation field was turned-off at 1 hr and it is clear that the oxalate species persist in solution. In terms of performing experimental validation, this case may be useful as it suggests that these species will remain in solution allowing them to be measured.

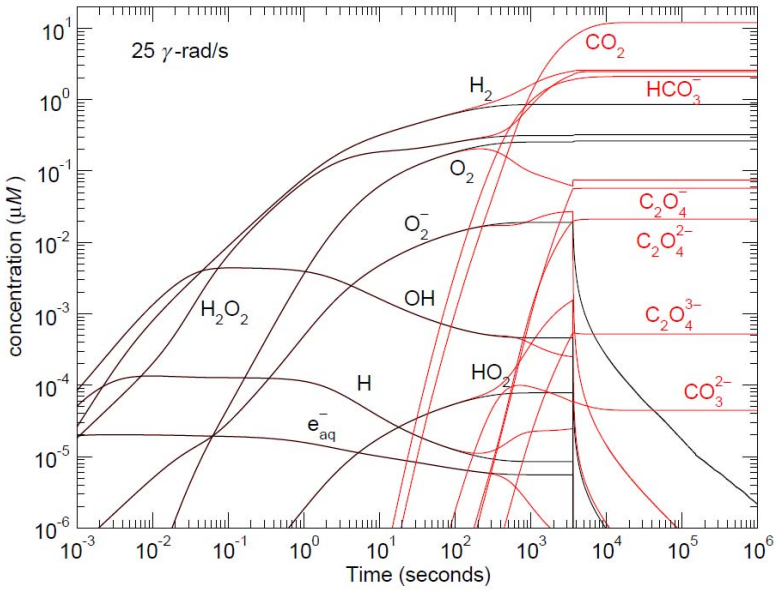

Figure 2.4 Occurrence of Oxalate during Water Radiolysis

2.4 UO_2 Corrosion rate

Once steady state conditions have been achieved the dissolution rate continues at a constant rate. This model was used to make comparison with the literature as the slope for UO_3D represents the corrosion rate. Figure 2.5 shows the dissolution rate for uranium oxide with a variable dose. The concentration of peroxide correlates strongly with the final dissolution rate.

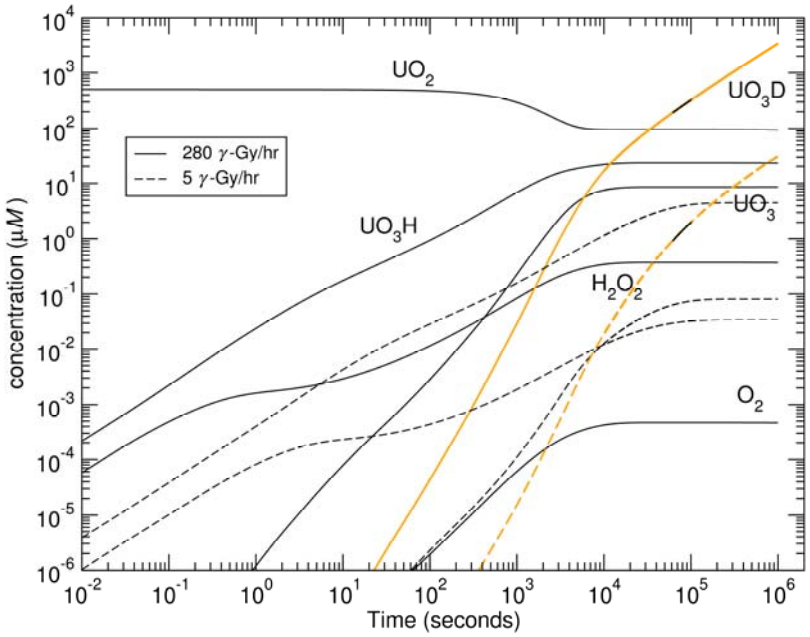

Figure 2.5 Predicted dissolution rate with radiolysis model

2.5 Flow-Through Testing

In the single pass flow through test (SPFT), crushed fuel or UO_2 specimens with a known surface area are contacted by a solution that passes at a known flow rate and at a constant temperature through the column containing the uranium oxide/fuel solid sample. The concentration of uranium (U) in the effluent solution exiting the sample cell is used to calculate the amount of solid fuel or UO_2 that has dissolved. The flow rate is determined by dividing the mass of solution that is collected for analysis by the duration over which it was collected.

The current radiolysis model uses as its basis the reactions for a water and uranium system produced by Christensen and Sunder (2000). Specifically, those assumptions are that the average behavior of fuel corrosion can be modeled with a single monomolecular layer of UO_2 reacting with chemical species within one diffusion length of the fuel. The uranium reactions included reflect the current thinking that the UO_2 surface first oxidizes to $UO_{2.33}$, and then dissolution of this surface (U^{VI}) occurs at a constant rate. The model has now been adapted to model flow through tests in which case the cell is a continuously stirred (diluted) reactor. It is a 2-region system in which the first region is a stagnant boundary layer with length scale on the order of the diffusion length of radiolytically produced radicals (30 μm). The second region represents the bulk aqueous solution that flows through the test column. Thus, only the second region is diluted by the inlet solution. Diffusion is also possible across the regions.

Previously under Christensen and Sunder (2000), the dissolution rate (normalized to surface area) was calculated from the slope of the concentration of UO_3D [$\mu M\ s^{-1}$] at steady state multiplied by the thickness [cm] of the monolayer:

$$DR\left[\frac{mg}{m^2 \cdot day}\right] = \lambda \frac{dC}{dt} C_1 = \lambda k[UO_3]\, C_1$$

Here, the conversion factor C_1 ensures the proper units for DR.

$$C_1 = 864 \cdot M_U$$

$$M_U = \text{atomic mass of U mixture in sample} \approx 238$$

In the current flow through test model, the concentration of UO_3D in the bulk (subscript *B*) can be expressed as:

$$\frac{dC_B^*}{dt} = k[UO_3] - \frac{R \cdot C_B^*}{V_B}$$

where C_B^* denotes that a mass imbalance is actually occurring because the reaction on UO_3 in region 1 is directly leading to the production of UO_3D in region 2, in which the volumes are different. However, this is okay because it does not require us to know the surface area since we are already normalizing DR to the surface area. Also, UO_3D only appears in the single reaction from UO_3, so concentrations of other species are not being affected. Since region 1 is then being modeled in the exact same way as Christensen and Sunder (2000), where the equation can be substituted into the equation above taken at steady state, and solved for DR:

$$DR\left[\frac{mg}{m^2 \cdot day}\right] = \frac{\lambda \cdot R \cdot C^*}{V_B} C_1$$

Experimentally (or by preserving mass balance), this would look like:

$$DR\left[\frac{mg}{m^2 \cdot day}\right] = \frac{R \cdot C_B}{A} C_1$$

Flow through results for UO_3D concentration for the dose rates of 0, 5, and 50 Gy/hr are shown in Figure 2.6. The red curve at 50 Gy/hr gives a dissolution rate reported by Gray et al. (1992) of about 5 mg/d•m^2.

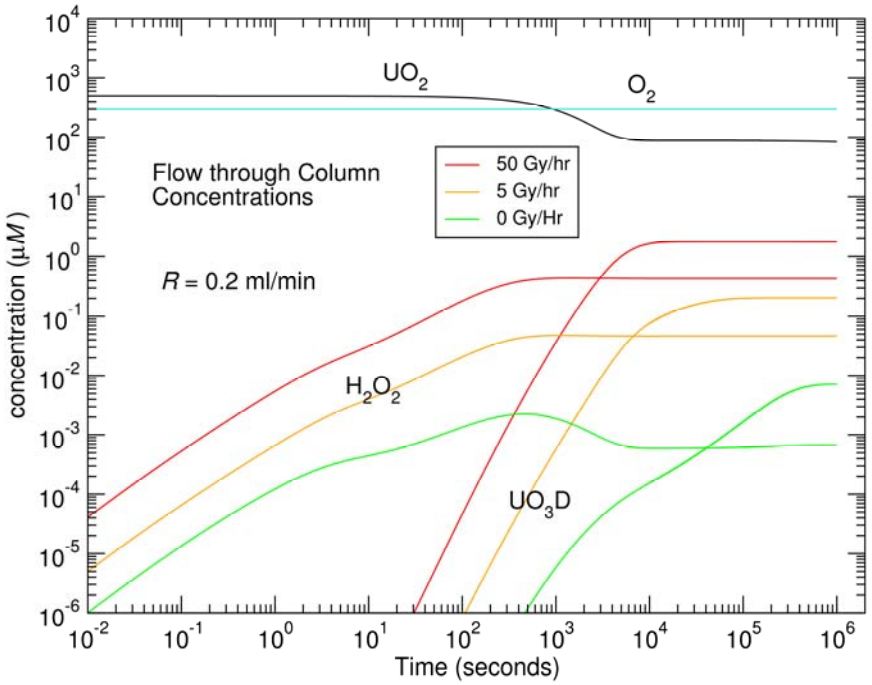

Figure 2.6 Predicted dissolution UO_2 rate (termed UO_3D), H_2O_2 production at a range of doses for the SPFT model

Figure 2.6 shows our predicted dissolved uranium concentration based on Christensen and Shoesmith (1994) kinetics adapted to the experimental conditions of a SPFT column as described by Gray et al. (1992). Conditions included a 0.2 ml/min flow of 0.02 M carbonate with p(20%) dissolved of O_2 through approx 200 mg of 33 MWd/kgU of Spent Fuel (Approved Testing Material (ATM)-103). The idealized model predictions show a steady state concentration of radiolytic products (e.g. H_2O_2) and dissolved uranium within several hours. The production of H_2O_2 for the zero dose case results from the reaction of O_2 with UO_2 and water.

Table 2.3 Uranium dissolution rates with γ Dose

Dose (Gy/hr)	Dissolution rate (mg/d•m^2)
0	0.021
5	0.59
10	1.1
50	6.0
100	9.5

We find that the measured dissolution rates of approximately 6 mg/d•m^2 of Gray et al. (1992) require a localized dose rate of about 50 Gy/hr. Depending on the precise geometry, this is consistent even with the ^{137}Cs gamma dose expected from 33 MWd/kgU Spent Fuel with a 10 yr decay time. Table 2.3 shows the dose dependence of our calculated dissolution rates for Gray et al. (1992) flow conditions. These results

mean that the observed dissolution rate was almost entirely due to short-lived radioactive species that would not be present in the material after 300 yrs.

2.6 FACSIMILE Modeling

The FACSIMILE program was originally developed to understand radiolysis in gas-cooled nuclear reactors, and it has since been updated to handle a large variety of fast chemical processes. Modeling in FACSIMILE can be most easily performed using the supplied Model Wizard. For example, the "*Create Base Model for Homogeneous Chemical Reaction Scheme*" wizard application takes information on the chemical reactions, rate constants, and initial species amounts to be considered and generates code that can then be run to obtain data on concentration versus time. Problems with the chemical database can occur if both reactants and products have +/- charges.

Although FACSIMILE provides a graphing wizard to help plot resulting data, there was a maximum allowance of 2,000 data points per plot. To plot more than one species on the same set of axes, either the amount of data must be limited or the specific time-period of interest needs to be constrained. Otherwise, an alternative means for plotting the data needs to be used. Larger volumes of data were plotted using Igor Pro. Data can be transferred to Igor following the steps given below:

1. Open and run the model to plot data.
2. Specify export to Excel via the File -> Export -> Export to Excel -> Setup Export menu options.
3. Re-save the .xls file created to the updated .xlsx file type (also remove any quotes around the filename).
4. Import this data into an Igor table through Data -> Load Waves -> Load Excel File menu options.
5. Choose a column of data to plot via the Windows -> New Graph option. Note: specify what data needs to be plotted on each axis.
6. Add data from other species to the graph by right-clicking on the graph window and choosing Append Traces to Graph. Note: this may need to be repeated until all data is shown on one set of axes.

To change the rate constants and initial amounts of reactant species, the basic syntax of the FACSIMILE code needs to be edited. Forward rate constants are labeled K#f while the reverse rate constants are labeled K#r, where # indicates the order of the chemical reactions entered. The code follows a traditional "*ConstantName ConstantValue*" order. For instance, if there are three reactions specified all with forward and backward rate constants then these constants would appear in the code as:

```
PARAMETER
K1f  1.43E11 K1r  2.574E-5 K2f  3.56E-2 K2r  2E10 K3f  2 K3r  0
;
```

where PARAMETER informs the program that these values are constants. Initial conditions are always assigned under a COMPILE INSTANT call and may be changed manually by the user.

2.6.1 FACSIMILE Test 1

To compare the FACSIMILE program against the code developed at PNNL, a pure-water scenario was evaluated. The first 31 equations provided by Christensen and Sunder (2000) were used for the FACSIMILE model. The corresponding code for this program is given below. Note that only the initial concentrations of H_2O and H_2O_2 were stated.

```
* Generated by FACSIMILE Reaction Wizard -
29 June 2011 ;
*========================================================= ;
* Christensen and Sunder- try 3 of water equations only.   ;
*========================================================= ;

EXECUTE OPEN 8 "C:\FACSIM~1\try3.out";

PARAMETER
K1f  3.4E7  K2f  2.7E7  K3f  9E9  K4f  1.8E10  K5f  2E10  K6f  1.9E10 K7f  1.2E10  K8f  1.3E10  K9f  2.2E10
K10f  2E1  K11f  3.5E9 K12f  7.9E9  K13f  5.5E9  K14f  2E10  K15f  6E7  K16f  1.5E7 K17f  9.6E7  K18f  8.4E5
K19f  4.5E10  K20f  8E5  K21f  2E10 K22f  3.56E-2  K23f  1.2E10  K24f  9.3E7  K25f  1.43E11 K26f  2.574E-5 K27f
3E10  K28f  2E10  K29f  1E10  K30f  2.5E10  K31f  5E9 ;

PERMIT +- ;
VARIABLE
E-        H         H+        H2        H2O       H2O2      HO2
HO2-      O-        O2        O2-       OH        OH-       ;

COMPILE INSTANT;
E- = 0 ;
H = 0 ;
H+ = 0 ;
H2 = 0 ;
H2O = 55.6 ;
H2O2 = 0.0002 ;
HO2 = 0 ;
HO2- = 0 ;
O- = 0 ;
O2 = 0 ;
O2- = 0 ;
OH = 0 ;
OH- = 0 ;
**;

COMPILE EQUATIONS ;
% K1f  : OH + H2 = H + H2O;
% K2f  : OH + H2O2 = HO2 + H2O;
% K3f  : OH + O2- = O2 + OH-;
% K4f  : H + O2 = HO2;
% K5f  : H + O2- = HO2-;
% K6f  : E- + O2 = O2-;
% K7f  : E- + H2O2 = OH + OH-;
% K8f  : E- + OH- + H2O = HO2- + OH-;
% K9f  : E- + H+ = H;
% K10f  : E- + H2O = H + OH-;
% K11f  : E- + HO2- = O- + OH-;
% K12f  : OH + HO2 = H2O + O2;
% K13f  : OH + OH = H2O2;
% K14f  : H + HO2 = H2O2;
% K15f  : H + H2O2 = H2O + OH;
% K16f  : H + OH- = E- + H2O;
% K17f  : HO2 + O2- = O2 + HO2-;
% K18f  : HO2 + HO2 = H2O2 + O2;
% K19f  : H+ + O2- = HO2;
% K20f  : HO2 = H+ + O2-;
% K21f  : H+ + HO2- = H2O2;
% K22f  : H2O2 = H+ + HO2-;
% K23f  : OH + OH- = H2O + O-;
% K24f  : O- + H2O = OH + OH-;
% K25f  : H+ + OH- = H2O;
% K26f  : H2O = H+ + OH-;
% K27f  : E- + OH = OH-;
% K28f  : H + OH = H2O;
% K29f  : H + H = H2;
% K30f  : E- + H + H2O = H2 + OH-;
% K31f  : OH + HO2- = HO2 + OH-;
**;

SETPSTREAM 1 8 ;
TIME ;
E-        H         H+        H2        H2O       H2O2      HO2       ;
HO2-      O-        O2        O2-       OH        OH-        ;
**;
```

```
COMPILE OUT ;
PSTREAM 1 ;
**;

WHENEVER TIME=
 1001 * (+1E2) 1E-4  %
CALL OUT;
**;

BEGIN;
STOP;
```

The initial concentrations given in the COMPILE INSTANT block may be changed at will by the user. This allows for ease of testing a multitude of different scenarios. FACSIMILE remains consistent with those units when balancing the equations as long as units are kept consistent throughout the process. If the provided database is used to search for chemical equations in the model, the correct units for the rate constant need to be chosen. In some instances, certain units may not be available through the database, and so equations and rate constants will need to be entered manually. Also, it is important to check the WHENEVER statement to make sure that no more than 5,000 different time stamps are being requested. The program will not compile otherwise. The best method for viewing the data was found to be by exporting the .out file to Microsoft Excel.

The PNNL developed code was then used to check that the FACSIMILE model was working correctly. The same initial conditions for region 1 were specified in the file rad-diff.in as in the FACSIMILE model which included changing the dose rate to 0 Gray/hr, the flow volume to 1, and flow rate (R) to 0. The rate constants for the reactions $H_2O_2 \rightarrow H_2O + O$ and $O + O \rightarrow O_2$ were also changed to zero as well in the file rate-const.txt in order to be consistent with the first 31 equations used in the FACSIMILE model. Upon running the program it was found that the steady-state values agreed with those values obtained from FACSIMILE for H^+, H_2O, H_2O_2, HO_2^-, and OH^-. Future work on this program will include:

- The use of dummy variables in the model of the decomposition of water.
- Splitting up the program to run the same model on different time intervals to gather more data- FACSIMILE.
- Incorporating the dose rate and G values into the model.
- Expanding the model to include the dissolution of UO_2.
- Incorporating sufficient graphing capabilities either in Igor Pro or Matlab.

3. Development of Simulant Fuels

Radiolytically-aged doped (RAD) synthetic nuclear fuels (RADFUELs) enable control of aging, radiolysis field, internal damage, microstructure, and phase distribution to allow establishment of the mechanisms of fuel corrosion. Synthetic fuels material irregularity may result in contradictory corrosion results, owing to changes in phase distribution, phase relationships, grain size, and oxidation states. A mixed oxide (MOX) solid has been made available for testing in this program and this was examined with SEM and EDS this past month. Figure 3.1 and Figure 3.2 show two MOX materials. There were numerous voids and precipitates in the material and they were found to be slightly inhomogeneous. There were isolated regions where the plutonium concentration was high. Neither of these materials was exposed to irradiation. Sufficient material is available for use in the corrosion tests. These materials will provide an internal alpha irradiation field.

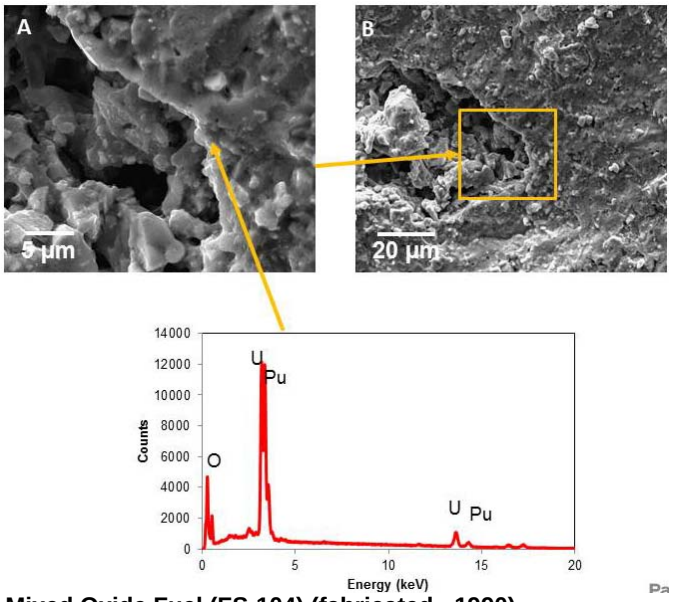

Figure 3.1 SEM analysis of Mixed Oxide Fuel (FS-104) (fabricated ~1990)

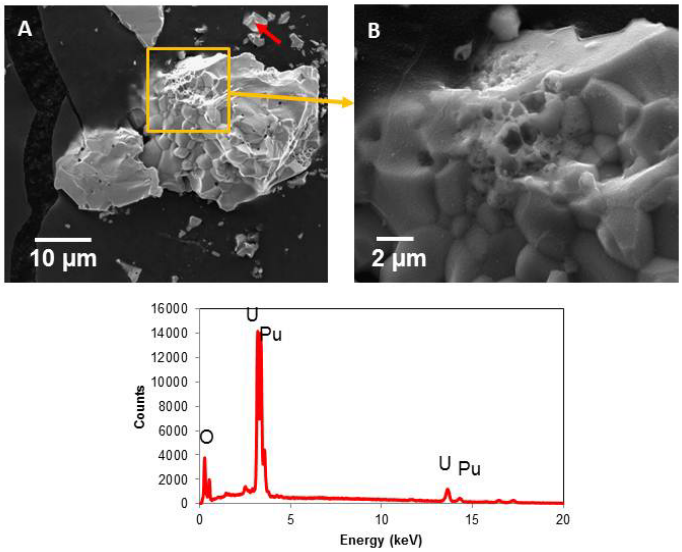

Figure 3.2 SEM analysis of Mixed Oxide Fuel (FS-9102-2) (fabricated ~1990)

3.1 Preparation of Synthetic Fuels

Radiolytically-aged doped (RAD) synthetic nuclear fuels (RADFUELs) allow control of aging, radiolysis field, internal damage, microstructure, and phase distribution to enable us to establish the true mechanisms for fuel corrosion. One problem with synthetic fuels material irregularity can result in contradictory corrosion results, owing to changes in phase distribution, phase relationships, grain size, and oxidation states. RADFUELs as defined will not be available to this project, so a series of synthetic UO_2 materials will be prepared and characterized for grain size distribution and phase distribution before testing. Table 3.1 describes some of the formulations and compositions of RADFUELs that would be a more accurate representation of actual aged fuels.

The synthetic fuels will also help us examine the behavior of elements that are usually at very low concentrations in spent fuels, such as Se and Np. The extremely low concentrations of some elements in actual fuels prevent an accurate characterization and elucidation of the chemistry in corrosion tests. Radiolysis plays a vital role in determining the alteration phases that form during Fuel corrosion and, subsequently, the extent that sequestration of key radionuclides (e.g., ^{99}Tc and ^{237}Np) is possible. Hughes-Kubatko et al. (2003) have calculated that the α-dose from natural uraninite was sufficient, under thin film conditions, to create enough peroxide for studtite to be stable. The α-dose from Used Fuel will be significantly higher, so the formation of uranyl peroxide phases may play a significant role in sequestering key radionuclides if the temperature is low enough to prevent decomposition.

Table 3.1 Example Compositions of Simulated Aged RADFUEL

OXIDE	SIMULATED 30 YR USED FUEL (SIM-0)	300 YR USED FUEL (SIM-300)	1000 YR USED FUEL SIM-1K
UO_2	97.43	97.43	97.40
ThO_2	0.10	0.10	0.099
ZrO_2	0.33	0.33	0.33
MoO_3	0.34	0.34	0.34
PdO	0.13	0.13	0.13
SrO	0.15	0	0
$BaCO_3$	0	0.25	0.25
Y_2O_3	0.04	0.14	0.22
CeO_2	0.30	0.30	0.30
La_2O_3	0.10	0.10	0.10
RuO_2	0.36	0.36	0.34
ReO_2	0.02	0.02	0.02
Nd_2O_3	0.48	0.48	0.47

3.2 Alteration of UO_2

An example of the effect of H_2O_2 on UO_2 is shown in Figure 3.3 where a characteristic alteration phase (studtite) has formed on the surface of the UO_2. The alteration phases (yellow) are 20-40 μm thick.

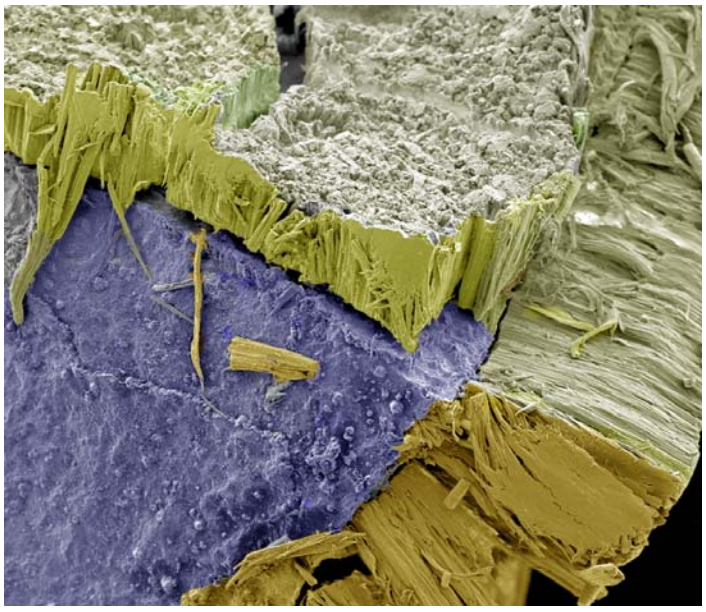

Figure 3.3 Colorized SEM image of Studtite on the surface of UO_2

4. Discussion and Future Work

The solubility and mobility of U is known to be strongly influenced by its oxidation state, which in turn is dependent on the mineralogy and solution composition. Under reducing conditions where U(IV) is stable, U forms sparingly soluble minerals such as uraninite (UO_2) and coffinite ($USiO_4$). If reducing conditions are maintained, U(IV) will be orders of magnitude less soluble than U(VI). The effect of radiolysis on the dissolution rate of Used Fuel will be examined using MOX solids and simulant RADFUELs doped with various levels of radionuclides and radionuclide simulants. The tests will be used to establish the magnitude of the radiolysis effect on fuel alteration, RN mobilization, and interactions with repository materials, including corroded Zircaloy and FeO_x. Static "bathtub and low-flow," and thin film (vapor) tests can be performed to cover the wide range of conditions the fuel may experience under a reducing geologic environment. Samples will be examined with a variety of microscopic and spectroscopic tools. Collaboration with Argonne National Laboratory (ANL) on spectroscopic characterization at the Advanced Photon Source will also be performed.

Tasks will continue to investigate the role of radiolysis on waste form degradation. These tasks will include the development of a user-friendly radiolysis modeling program for simulating complex environments. Validation tests will be performed over the range of repository-relevant conditions to accurately assess the role of radiolysis in waste form degradation and radionuclide release. We will also collaborate with ANL by seeing if specific tests conducted at ANL may be useful to model. To have more effective control over the properties of the uranium oxide solids in the tests, unirradiated UO_2 doped can be used with various levels of radionuclides. These ceramics are termed radiolytically aged doped synthetic nuclear fuels (RADFUELs), which will help us elucidate the effect of doping on the fuel chemistry and the radiolysis effect. MOX materials will also be tested for H_2O_2 and H_2 formation and alteration.

The objective of the combination of modeling and testing will be to try to separate out the β,γ field from the long-term α-field. This will lead to more reasonable long-term corrosion rates for Used Fuel and a more defensible generic Used Fuel dissolution model.

5. References

Bruno, J., L. Duro, and M. Grivé, 2002. "The applicability and limitations of thermodynamic geochemical models to simulate trace element behaviour in natural wasters. Lessons learned from natural analogue studies." *Chemical Geology* 190:371-393.

Buck, E.C., P. A. Finn, and J. K. Bates, 2004. "Electron energy-loss spectroscopy of anomalous plutonium behavior in nuclear waste materials." *Micron* 35/4:235-243.

Carbol, P., Fors, P., van Winkel, S., and K. Spahiu, 2009. "Corrosion of irradiated MOX fuel in presence of dissolved H_2," *Journal of Nuclear Materials*, 392: 45-54.

Christensen, H., and D.W. Shoesmith, 1994. "Oxidation of nuclear fuel (UO_2) by the products of water radiolysis: development of a kinetic model," *Journal of Alloys and Compounds,* 213/214: 93-99.

Christensen, H. and S. Sunder, 2000. "Current state of knowledge of water radiolysis effects on spent nuclear fuel corrosion." *Nuclear Technology* 131: 102-123.

Finch, R. J. and R. C. Ewing, 1992. "The corrosion of uraninite under oxidizing conditions," *Journal of Nuclear Materials*, 190: 133-156.

Finch, R.J., Buck, E.C., Finn, P.A., J.K. Bates, 1999. "Oxidative corrosion of spent UO_2 fuel in vapor and dripping groundwater at 90°C", Material Research Society Symposium Proceedings. 556: 431-438

Finn, P. A., R. J. Finch, E. C. Buck, and J. K. Bates, 1998. "Corrosion mechanisms of Spent Nuclear Fuel under oxidizing conditions." *Materials Research Society Symposium Proceedings* 506:123-131.

Gray, W. J. and G. L. McVay, 1985. "Nitric acid formation during gamma irradiation of air/water mixtures*," Radiation Effects*, 89: 257-262.

Gray, W. R., Leider, H.R. and S.A. Steward, 1992. "Parametric study of LWR spent fuel dissolution kinetics," *Journal of Nuclear Materials*, 190: 46-52

Hanson, B., McNamara, B., Buck, E., Friese, J., Jenson, E., Krupka, K., and B. Arey, 2005. "Corrosion of commercial spent nuclear fuel: 1. Formation of studtite and metastudtite," Radiochemica Acta, 93: 159-168.

Hughes-Kubatko, K-A., K. B. Helean, A. Navrotsky, and P.C. Burns, 2003. "Stability of peroxide-containing uranyl minerals." *Science* 302:1191-1193.

King, F., M. Kolar, and D. W. Shoesmith, 1999. "Modeling the oxidative dissolution of UO_2." *Materials Research Society Symposium Proceedings* 556:463-470.

LaVerne, J. A., and L. Tandon, 2002. "H_2 Production in the Radiolysis of Water on UO_2 and Other Oxides," *Journal of Physical Chemistry* B107: 13623-13628.

Li, C. and D. R. Olander, 1999. "Steam radiolysis by alpha-particle irradiation," *Radiation Physics and Chemistry*, 54: 361-371.

Pastina, B., and J. A. LaVerne, 2001. "Effect of Molecular Hydrogen on Hydrogen Peroxide in Water Radiolysis," *Journal of Physical Chemistry* A105: 9316-9322.

Pérez del Villar, L., J. Bruno, R. Campos, P. Gómez, J. S. Cózar, A. Garralón, B. Buil, D. Arcos, G. Carretero, J. Ruiz Sánchez-Porro, and P. Hernán, 2002. "The uranium ore from Mina Fe (Salamanca, Spain) as a natural analogue of processes in a Used Fuel repository." *Chemical Geology* 190:395-415.

Petrik, N. G., A. B. Alexandrov, and A. I. Vall. 2001. "Interfacial Energy Transfer during Gamma Radiolysis of Water on the Surface of ZrO_2 and Some Other Oxides." *Journal of Physical Chemistry* B105: 5935-5944.

Poinssot, C. Ferry, C. M. Kelm, B. Grambow, A. Martinez, A., Johnson, L., Andriamoloolona, Z., Bruno, J., Cachoir, C., Cavedon, J.M., Christensen, H., Corbel, C., Jegou, C., Lemmens, K., Loida, A., Lovera, P., Miserque, F. de Pablo, J., Poulesquen, A., Quinones, J. Rondinella, V., Spahiu, K., and D. H. Wegen, 2005. Spent Fuel Stability under Repository Conditions: Final Report of the European Project, European Commission, 5th EURATOM FRAMEWORK PROGRAMME, 1998-2002.

Shoesmith, D.W., 2000. "Fuel corrosion processes under waste disposal conditions." *Journal of Nuclear Materials* 282:1-31.

Spahiu, K., U.-B. Eklund, D. Cui, and M. Lundström, 2002. "The influence of near-field redox conditions on Spent Fuel leaching." *Materials Research Society Symposium Proceedings* 713:633-638.

Sunder, S., D. W. Shoesmith, and N. H. Miller, 1997. "Oxidation and dissolution of nuclear fuel (UO_2) by the products of the alpha radiolysis of water." J*ournal of Nuclear Materials* 244:66-74.

Vladimirova, M. V., and Kulikov, I. A. 2002. "Formation of H_2 and O_2 in Radiolysis of Water Sorbed on PuO_2," *Radiochemistry*, 44, 83-86.

ACKNOWLEDGEMENTS

This work was supported by the US Department of Energy, Office of Nuclear Energy, Used Fuel Disposition (UFD) – Repository Science (RS) Program under Contract. Pacific Northwest National Laboratory is operated for the U.S. Department of Energy by Battelle under Contract DE-AC05-76RL01830.